Constraining light-driven plasticity in leaf traits with observations improves the prediction of tropical forest demography, structure, and biomass dynamics

Yixin Ma[1,*], Paul R. Moorcroft[2], S. Joseph Wright[3], Alistair Rogers[4,8], Julien Lamour[5,8], Kenneth J. Davidson[8], Shawn P. Serbin[6,8], Matteo Detto[3,7], Xiangtao Xu[1,*]

[1] Department of Ecology and Evolutionary Biology, Cornell University, Ithaca, NY 14850

[2] Department of Organismic and Evolutionary Biology, Harvard University, Cambridge, MA 02138

[3] Smithsonian Tropical Research Institute, Apartado 0843–03092 Balboa, Republic of Panama

[4] Climate & Ecosystem Sciences Division, Lawrence Berkeley National Laboratory, Berkeley, CA 94720

[5] Centre de Recherche sur la Biodiversité et l'Environnement (CRBE), Université de Toulouse, CNRS, IRD, Toulouse INP, Université Toulouse 3 – Paul Sabatier (UT3), Toulouse, France

[6] Biospheric Sciences Laboratory, NASA Goddard Space Flight Center, Greenbelt, MD, 20771

[7] Department of Ecology and Evolutionary Biology, Princeton University, Princeton, NJ 08542

[8] Environmental and Climate Sciences Department, Brookhaven National Laboratory, Upton, NY 11973

[*] To whom correspondence may be addressed.

Corresponding author: Yixin Ma (ym524@cornell.edu); Xiangtao Xu (xx286@cornell.edu)

Word count: 7064

Number of figures: 8

Number of tables: 2

Supplementary information: Figures S1-S5, Table S1

Key Points:

- We examined how intra-specific light plasticity in leaf traits affects modeled tropical tree demography and long-term forest dynamics.
- Observation-constrained light plasticity enabled an accurate prediction of tree growth rates, forest structure, and biomass regrowth.
- Light plasticity improved modeled forest composition and trait diversity, which cannot be achieved by adding new plant functional types.

Abstract

Predicting tropical tree demography is a key challenge in understanding the future dynamics of tropical forests. While demographic processes are known to be regulated by leaf trait diversity, only the effect of inter-specific trait variation has been evaluated, and it remains unclear as to what degree the intra-specific trait plasticity across light gradients (hereafter light plasticity) regulates tree demography, and how this will further shape long-term community and ecosystem dynamics. By combining *in situ* trait measurements and forest census data with a terrestrial biosphere model, we evaluated the impact of observation-constrained light plasticity on demography, forest structure, and biomass dynamics in a Panamanian tropical moist forest. Modeled leaf physiological traits vary across and within plant functional types (PFT), which represent the inter-specific trait variation and the intra-specific light plasticity, respectively. The simulation using three non-plastic PFTs underestimated 20-year-average understory growth rates by 41%, leading to a biased forest size structure and leaf area profile, and a 44% underestimate in long-term biomass. The simulation using three plastic PFTs generated accurate understory growth rates, resulting in a realistic forest structure and a smaller biomass underestimate of 15%. Expanding simulated trait diversity using 18 non-plastic PFTs similarly improved the prediction of demography and biomass. However, only the plasticity-enabled model predicted realistic long-term PFT composition and within-canopy trait profiles. Our results highlight the distinct role of light plasticity in regulating forest dynamics that cannot be replaced by inter-specific trait diversity. Accurately representing light plasticity is thus crucial for trait-based prediction of tropical forest dynamics.

Plain Language Summary

Ecosystem functions such as biomass dynamics and forest structure are strongly regulated by plant diversity. In addition to species diversity, plant characteristics also vary within the same species, particularly in response to environmental gradients. However, it remains largely unclear how this intra-specific diversity across environmental gradients regulates forest dynamics. Here we used vegetation modeling to investigate how the intra-specific diversity across different light environments regulates tropical tree demography, forest

composition, and carbon cycle. We found that incorporating intra-specific diversity in the model substantially influenced tree growth rates, forest structure, and long-term carbon accumulation. Constraining intra-specific diversity with observations improved model predictions of these processes. In addition, incorporating the intra-specific diversity improved the prediction of forest composition, and such an effect cannot be replaced by solely incorporating higher species diversity. These results highlight the importance of characterizing the intra-specific diversity across environmental gradients for predicting long-term tropical forest dynamics.

1 Introduction

The future fate of tropical forests, particularly the persistence of old-growth forest carbon sink and the regrowth potential of secondary forests, critically influences the global carbon cycle, biodiversity, and the realization of several Sustainable Development Goals (Anderson-Teixeira et al., 2016; Pan et al., 2011; United Nations General Assembly, 2015). Predicting the community and ecosystem dynamics of these forests fundamentally depends on a realistic representation of demographic processes such as growth and mortality. However, accurately predicting tropical tree demography remains an open challenge for process-based terrestrial biosphere models (TBM), and a common modeling bias is the underestimate of the abundance of understory trees (Koven et al., 2020; Longo et al., 2019a), which can lead to further biases in the prediction of long-term canopy regeneration and forest succession.

Understory trees in closed-canopy tropical forests are limited by low light availability (Chazdon & Fetcher, 1984; Clark et al., 1996), thus their demographic rates are strongly regulated by the diversity in light use-associated traits (Denslow, 1987; Detto et al., 2021; Finegan, 1984; Moorcroft et al., 2001). The inter-specific variation in these traits, particularly the trait variation between light-demanding and shade-tolerant species, has been shown to influence demographic rates and ecosystem functioning (Reich, 2014; Wright et al., 2010). In addition to the inter-specific variation, leaf traits within the same species also vary substantially across light gradients in tropical forests (Xu et al. 2017). This intra-specific trait variation largely

results from phenotypic plasticity in response to within-canopy light gradients (hereafter light plasticity), although ontogeny and other environmental factors also contribute to the variation (Cavaleri et al., 2010; Coste et al., 2009; Dang-Le et al., 2013; Detto & Xu, 2020; Wen et al., 2008). To date, it has not been evaluated as to what degree light plasticity regulates understory tree demography in tropical forests.

Both light plasticity and inter-specific variation enhance functional diversity and thus are expected to influence forest dynamics, but light plasticity can affect ecosystem processes through two unique mechanisms. First, it can increase net carbon gain in the understory by reducing respiration cost and increasing specific leaf area (Niinemets et al., 2015; Poorter et al., 2019), which can directly increase tree fitness during their early life stages and thus enhance their growth, survival, and abundance. In contrast, inter-specific trait variation can not lead to tree-level trait adjustments within their lifetime. Second, the inter-specific trait variation characterizes the tradeoff between growth in high light environment and survival in low light environment, whereas plasticity-enabled trait variation weakens such tradeoff by increasing understory survival (Sterck et al., 2013). Based on these mechanisms, light plasticity is expected to shape demographic processes and community composition differently than the inter-specific trait variation.

In TBMs, the inter-specific trait variation is often modeled as plant functional types (PFT), which are groups of species with similar trait values, and light plasticity has been commonly represented as intra-PFT trait variation across light gradients. While many studies have aimed to improve the model representation of inter-PFT variation (Butler et al., 2022; Pappas et al., 2016; Pavlick et al., 2013; Rius et al., 2023; Sakschewski et al., 2016), fewer studies have attempted to refine the representation of plasticity and evaluate its impact on predicting forest dynamics (Needham et al., 2025). In fact, TBMs often incorrectly assume that the extent of light plasticity is identical across different PFTs and traits (see **Table 1** for a summary of light plasticity implementation in TBMs), despite field observations demonstrating that different species and traits exhibit a wide range of light plasticity (Chmura et al., 2017; Osunkoya et al., 1994; Valladares et al., 2000). For example, both leaf dark respiration rate and maximum carboxylation rate of photosynthesis (V_{cmax}) decrease with lower light levels, but leaf

dark respiration has a higher degree of plasticity than that of V_{cmax}, resulting in a lower respiration to V_{cmax} ratio (Lamour et al., 2023) and thus a higher shade tolerance in the understory. The absence of difference in modeled respiration and V_{cmax} plasticity likely explains the underestimate of understory abundance in plasticity-enabled TBMs (Koven et al., 2020; Longo et al., 2019a), and this is partly supported by previous research showing that a higher degree of leaf dark respiration plasticity in FATES model increases understory leaf area (Needham et al., 2025). However, it remains unknown whether a comprehensive and realistic representation of light plasticity, i.e., incorporating its variation across species and multiple traits, can fully correct for the model biases in understory growth and survival and further improve the prediction of long-term forest dynamics.

To examine the role of light plasticity in explaining and predicting tropical forest dynamics, we combined *in situ* trait measurements in Panama and forest inventories at Barro Colorado Island (BCI) with the Ecosystem Demography Model version 2.2 (ED2) (Longo et al., 2019b). The ED2 model is a trait-based, demography-enabled TBM, and it represents light plasticity in leaf physiological traits as intra-PFT parameter variation driven by light gradient. The modeled light plasticity is constrained by local observations, and the degree of light plasticity varies across PFTs and traits (**Table 1; Fig. 1**).

Overall, we expected that light plasticity would improve the prediction of forest structure and long-term forest succession by better capturing understory demography, and its effect would be different from that of inter-specific trait diversity. Specifically, we hypothesized that: (1) a non-plastic model containing only inter-PFT trait variation would underestimate growth rates and overestimate mortality rates in the understory, consequently underestimating tree abundance and leaf area; (2) incorporating observation-constrained light plasticity would yield more accurate demographic rates and thus a more realistic forest size structure and leaf area vertical profile; (3) during long-term secondary succession, light plasticity would promote forest biomass accumulation; (4) expanding inter-specific diversity in the non-plastic model by adding more PFTs would have a smaller positive effect on understory growth and long-term biomass than light plasticity.

148 **Table 1.** Current representation of light plasticity in TBMs and its impact on modeled ecological processes.

Model	Traits that have light plasticity	Do traits differ in light plasticity	Do PFTs differ in light plasticity	Ecological impact of light plasticity	Reference
Joint UK Land Environment Simulator (JULES)	V_{cmax}; J_{max}; Leaf dark respiration; Leaf nitrogen content;	No. All traits have the same plasticity.	No. All PFTs have the same plasticity	Small, positive effect on canopy photosynthesis	Mercado et al. 2007
Community Land Model version 4 (CLM4)	V_{cmax}; J_{max}; Leaf dark respiration; Leaf nitrogen content	No. All traits have the same plasticity.	No. All PFTs have the same plasticity.	Small, positive effect on gross primary productivity (GPP)	Bonan et al. 2011
Lund-Potsdam-Jena General Ecosystem Simulator (LPJ-GUESS)	$V_{cmax;}$ J_{max}; Leaf dark respiration; Leaf nitrogen content;	No. All traits have the same plasticity.	No. All PFTs have the same plasticity.	Not examined	Smith et al. 2014
Trait-based Forest Simulator version 2 (TFSv.2)	V_{cmax}; J_{max}; Leaf dark respiration; Specific leaf area; Leaf lifespan	Yes. The light plasticity of leaf lifespan is different from that of other traits.	No. All PFTs have the same plasticity.	Not examined	Fauset et al. 2019

149

Table 1. (continued)

Functionally Assembled Terrestrial Ecosystem Simulator (FATES)	V_{cmax}; J_{max}; Leaf dark respiration; Leaf nitrogen content; Specific leaf area	Yes. Leaf dark respiration is the most plastic, and all other traits have the same plasticity.	Yes. Early-successional PFT is the most plastic.	Positive effect on leaf area and vegetation carbon	**Needham et al. 2025**
Organizing Carbon and Hydrology In Dynamic Ecosystems (ORCHIDEE)	V_{cmax}; J_{max}; Leaf dark respiration; Leaf nitrogen content	No. All traits have the same plasticity.	No. All PFTs have the same plasticity	Not examined	Zhang et al. 2020
Ecosystem demography Model version 2.2 (ED2)	**V_{cmax}; J_{max}; Leaf dark respiration; Specific leaf area; Leaf lifespan**	**Yes. Each trait plasticity is parameterized separately.**	**Yes. Early-successional PFT is the most plastic.**	**Large effect on tree demography, forest structure, composition, trait diversity, and biomass**	**This study**

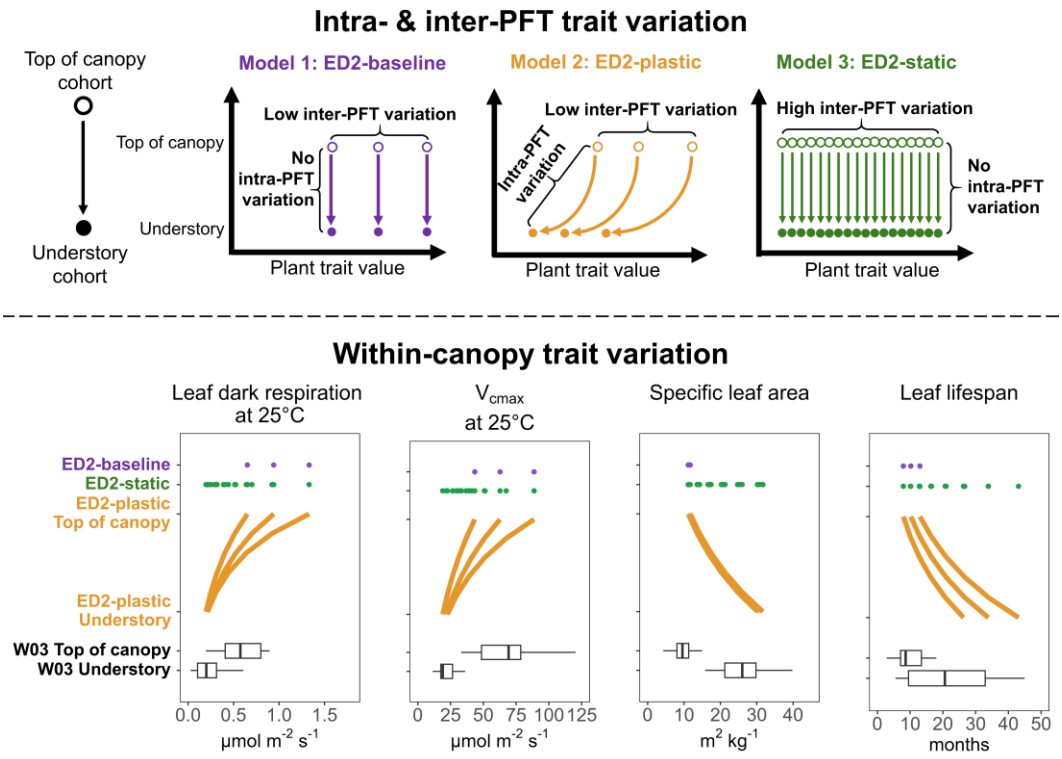

Figure 1. Representation of plant functional diversity in ED2 model for four traits of interest: leaf dark respiration rate at 25°C, maximum carboxylation rate of photosynthesis (V_{cmax}) at 25°C, specific leaf area, and leaf lifespan. The upper panel is a conceptual diagram of the different components of plant functional diversity in each model. Open and closed circles represent the trait variation between top-of-canopy cohorts and understory cohorts. ED2-baseline only contains trait variation across three PFTs, without intra-PFT variation. ED2-plastic contains both trait variation across three PFTs and intra-PFT light plasticity. ED2-static only contains trait variation across 18 PFTs, without intra-PFT variation. The lower panel shows the model parameterization of within-canopy trait variation. ED2-baseline, ED2-plastic, ED2-static are represented by purple, orange, and green colors, and each point or line represents a different PFT. Light plasticity in ED2-plastic was parameterized based on top-of-canopy and understory trait values from the W03 dataset (described in section 2.3 and 2.4). Although not shown here, simulated maximum rate of photosynthetic electron transport (J_{max}) in ED2 is proportional to V_{cmax} by a constant factor, therefore, it is also a plastic trait and it has the same light plasticity as V_{cmax}.

2 Materials and Methods

2.1 Study site

The study site is a long-term, 50-ha forest plot at Barro Colorado Island (BCI) in Panama. The BCI site is an old-growth moist tropical forest with a mean annual precipitation of 2660 mm

193 and a four-month dry season. The plot was established in 1981. The species identity, spatial
194 coordinates within the plot, and diameter at breast height (DBH) of all stems with DBH ≥ 1 cm
195 were first inventoried in 1982 and then recorded every five years since 1985 (Condit et al.,
196 2017).

197 2.2 Model description

198 The ED2 model is a cohort-based TBM that simulates vegetation dynamics and land
199 surface processes (Longo et al., 2019b). In this model, the smallest spatial unit is a patch, which
200 is a collection of areas with similar disturbance histories, and its size is usually comparable to a
201 forest gap (~20m). Within each patch, there are multiple cohorts, which are individuals of
202 similar size and same PFT. Each cohort is always shaded by all other taller cohorts within the
203 same patch, therefore, cohorts experience height-structured competition for light, which
204 further drives vegetation dynamics.

205 Cohort-level growth and mortality rates are simulated based on ecophysiological
206 principles and are tracked explicitly throughout the simulation. DBH growth rate is determined
207 by cohort-level net carbon balance, which is further governed by photosynthesis, respiration,
208 and carbon allocation among different plant compartments. The cohort-level mortality rate is
209 modeled as the sum of growth-independent and growth-dependent components and is
210 described by the following equation based on Camac et al. (2018).

211 $$\boldsymbol{M = M_b + M_d + \alpha * e^{\beta * growth}}, \quad (1)$$

212 $\boldsymbol{M}$ is the total cohort-level mortality rate. $\boldsymbol{M_b}$ is baseline mortality rate, and it is a
213 prescribed parameter that differs across PFTs. $\boldsymbol{M_d}$ is disturbance-related mortality, and it has
214 the same value for all PFTs. The last term in this equation describes the growth-dependent
215 mortality rate. $\boldsymbol{\alpha}$ and $\boldsymbol{\beta}$ are both PFT-dependent parameters, and $\boldsymbol{\beta}$ is always negative, meaning
216 that this growth-dependent mortality rate declines exponentially with larger DBH growth rates.

217 To isolate the effect of light plasticity and inter-specific trait variation, we generated
218 three ED2 versions that have different representations of intra-PFT light plasticity and inter-PFT

trait variation (**Fig. 1**). **ED2-baseline** characterizes three PFTs (described in section 2.5) that do not have light plasticity, meaning that traits do not vary with light levels. **ED2-plastic** has three plastic PFTs, and their traits respond to light gradients (described in section 2.3 and 2.4). **ED2-static** characterizes 18 PFTs that do not have light plasticity, but its inter-PFT trait variation covers a similar range of variation as the intra-PFT light plasticity in ED2-plastic (described in section 2.5).

2.3 Model representation of light-driven plasticity

Five leaf traits vary across cohorts and are modeled as plastic: leaf dark respiration rate, V_{cmax}, maximum rate of photosynthetic electron transport (J_{max}), specific leaf area (SLA), and leaf lifespan. These traits are selected because they are available in a local trait dataset (described in section 2.4) and they are important in determining leaf-level carbon balance and leaf turnover rates. The values of these plastic traits vary both across and within PFTs, and the intra-PFT variation across cohorts depends on the cohort-level overtopping leaf area index (oLAI). For each cohort of interest, oLAI is the total leaf area index (LAI) for all cohorts that grow in the same patch and are taller than the cohort of interest. Leaf area is modeled by a power-law function of DBH, and this function is estimated from the leaf area profile measured by LiDAR (light detection and ranging) at the BCI 50-ha plot (Detto et al., 2015). We used oLAI rather than absolute light levels to characterize the light environment for the following reasons. First, there was no direct measurement of the light environment at the BCI plot. Second, oLAI characterizes neighborhood shading, which is a major source of within-canopy light environment variation.

We assumed that plasticity-induced trait changes only occur with leaf turnover, i.e., the trait value of a new leaf is calculated based on the current oLAI (equation 2) and will then remain constant at the leaf level. The cohort-level trait value is an average across new and old leaves (equation 3), and there is no within-crown trait variation. As described previously, oLAI is calculated from DBH, which is updated monthly, thus cohort-level oLAI and trait values are both updated monthly.

246 The cohort-level trait value is calculated based on the following equations:

247 $$\boldsymbol{X_{i,j,new} = X_{i,0} * e^{k_i * oLAI_{i,j}}}, \quad (2)$$

248 $$\boldsymbol{X_{i,j,t+1} = \left(1 - \ turnover_{i,j,t}\right) * X_{i,j,t} + \ turnover_{i,j,t} * \ X_{i,j,new}} \quad (3)$$

249 The equation 2 is based on Lloyd *et al.* (2010). $\boldsymbol{X_{i,j,new}}$ is the trait value of a new leaf in
250 cohort *j* within PFT *i*. $\boldsymbol{X_{i,0}}$ is the trait value for a top-of-canopy cohort (oLAI=0) of PFT *i*. $\boldsymbol{k_i}$ is the
251 light plasticity coefficient for PFT *i*. $\boldsymbol{X_{i,0}}$ and $\boldsymbol{k_i}$ are prescribed parameters for each trait and
252 each PFT. $\boldsymbol{oLAI_{i,j}}$ is the light environment of cohort *j* within PFT *i*. The parameterization of $\boldsymbol{k_i}$ is
253 described in section 2.4, and the parameterization of $\boldsymbol{X_{i,0}}$ is described in section 2.5.

254 In equation 3, $\boldsymbol{X_{i,j,t+1}}$ is the cohort-level trait value at month *t+1*. $\boldsymbol{X_{i,j,t}}$ is the value at
255 month *t*. $\boldsymbol{turnover_{i,j,t}}$ is the leaf turnover rate of cohort *j* within PFT *i* at month *t*, and it is the
256 inverse of leaf lifespan (measured in the unit of month). Larger values of $\boldsymbol{turnover_{i,j,t}}$ suggest
257 that leaf turnover occurs at a faster rate and that traits more closely track changes in the light
258 environment.

259 2.4 Parameterization of PFT-level light plasticity

260 To parameterize the PFT-level light plasticity coefficient $\boldsymbol{k_i}$, we first calculated the
261 observed species-level light plasticity based on a trait dataset collected during 1999-2002 at the
262 San Lorenzo site and the Parque Natural Metropolitano site in Panama (hereafter W03 dataset;
263 more detail is available in Xu *et al.*, 2017). These sites are equipped with cranes that are 42 m
264 and 52 m, respectively. For 64 measured species, leaf samples were collected from both their
265 understory saplings and sun-exposed branches of top-of-canopy trees, and we assumed that
266 the measured vertical trait variation is completely explained by light plasticity. Neither height
267 nor light level was measured at the site of the sampling, so samples were labeled categorically
268 as “understory” (oLAI > 0) or “top-of-canopy” (oLAI = 0). Measured traits include SLA, leaf
269 lifespan, light-saturated leaf photosynthesis rate at ambient temperature, and leaf dark
270 respiration rate at ambient temperature. We calculated V_{cmax} at 25°C from the photosynthesis
271 rate using the FvCB photosynthesis model (Xu et al., 2017).

Based on equation 2, we generated the following equation to estimate species-level light plasticity:

$$\boldsymbol{k_p} = \frac{1}{\boldsymbol{oLAI_{und}}} \boldsymbol{log_e}\left(\frac{\boldsymbol{X_{p,und}}}{\boldsymbol{X_{p,toc}}}\right), \quad (4)$$

where $\boldsymbol{k_p}$ is the light plasticity coefficient of species *p*, $\boldsymbol{X_{p,und}}$ is the average understory leaf trait value of species *p*, $\boldsymbol{X_{p,toc}}$ is the average top-of-canopy leaf trait value of species *p*. We estimated $oLAI_{und}$ as 5 m^2 m^{-2} based on the measured leaf area profile at BCI (Detto et al., 2015). The across-species medians of $\boldsymbol{k_p}$ were -0.233, -0.227, 0.184, and 0.139 for leaf dark respiration rate, V_{cmax}, SLA, and leaf lifespan, respectively (**Fig. 2A**).

To parameterize PFT-level $\boldsymbol{k_i}$ from species-level $\boldsymbol{k_p}$, we analyzed the relationship between species-average, top-of-canopy traits and their $\boldsymbol{k_p}$ values (**Fig. 2B-2E**). We found that V_{cmax} plasticity was positively and linearly related to top-of-canopy V_{cmax} across species, so k_{vcmax} was parameterized as a linear function of top-of-canopy V_{cmax} (equation 5). Similarly, leaf dark respiration plasticity was parameterized as a linear function of top-of-canopy leaf dark respiration rate (equation 6).

$$\boldsymbol{k_{vcmax,i}} = -\left(\boldsymbol{0.00242 * V_{cmax\,i,0} + 0.06212}\right) \quad (5)$$

$$\boldsymbol{k_{resp,i}} = -\left(\boldsymbol{0.18974 * Respiration_{i,0} + 0.11744}\right) \quad (6)$$

Where $\boldsymbol{k_{vcmax,i}}$ is the V_{cmax} plasticity of PFT *i*, $\boldsymbol{V_{cmax\,i,0}}$ is the V_{cmax} at 25°C for a top-of-canopy cohort within PFT *i*. $\boldsymbol{k_{resp,i}}$ is leaf dark respiration plasticity of PFT *i*, $\boldsymbol{Respiration_{i,0}}$ is the leaf dark respiration at 25°C for a top-of-canopy cohort within PFT *i*. SLA plasticity and leaf lifespan plasticity were not significantly related to their top-of-canopy trait values, so we calculated the average k_{SLA} (0.199) and k_{LL} (0.240) across all species and assigned them to all PFTs. J_{max} in ED2 is modeled as proportional to V_{cmax} by a constant factor, therefore, we assumed that k_{Jmax} equals k_{vcmax} for all PFTs (**Table S1**).

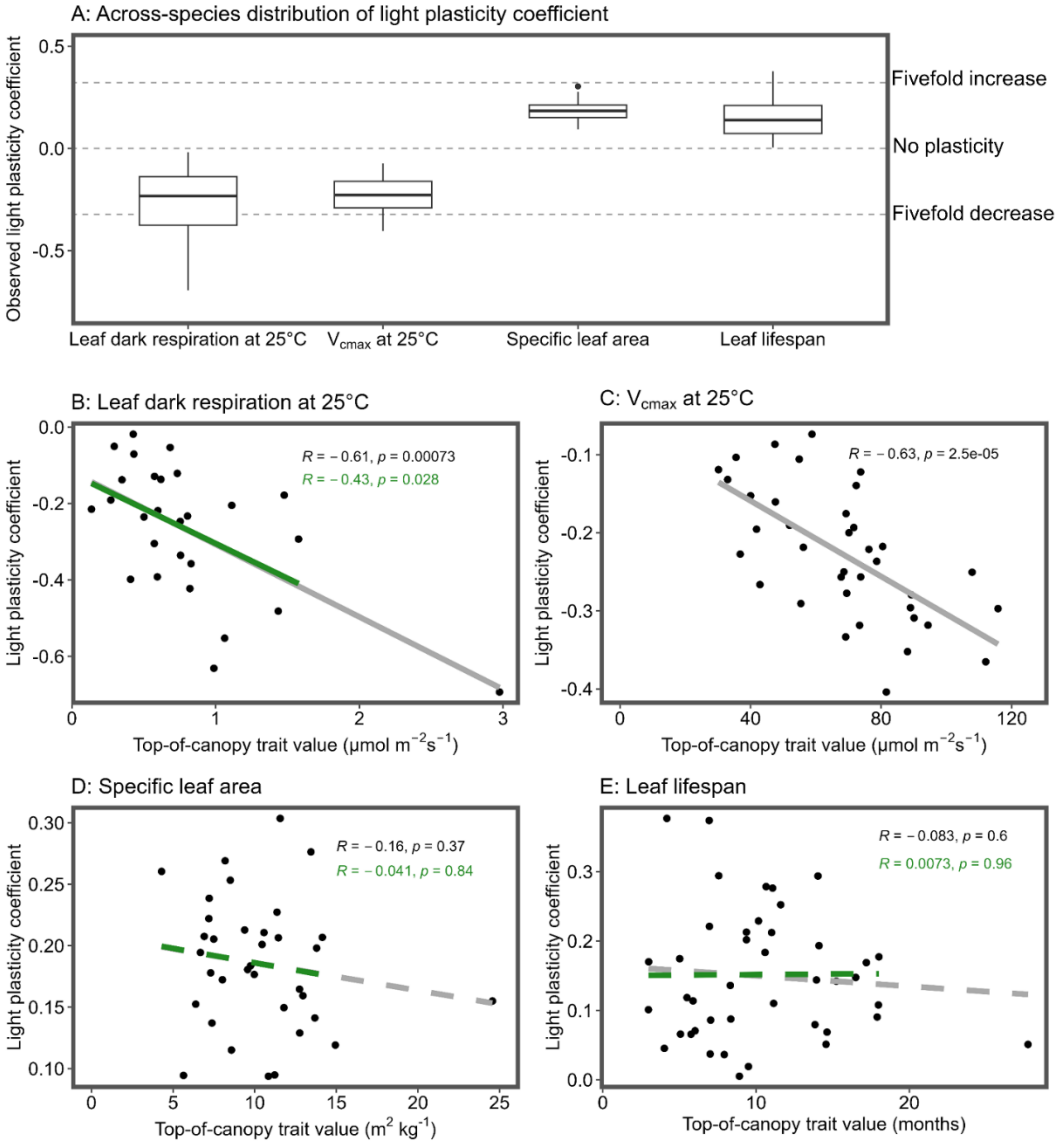

Figure 2. Species-level light plasticity of leaf dark respiration rate, V_{cmax}, specific leaf area, and leaf lifespan observed in the W03 dataset. (A) shows the distribution of species-level light plasticity coefficient (k_p in equation 4). Dashed horizontal lines indicate k_p values at which traits increase or decrease by fivefold across an oLAI gradient of 0-5 $m^2\ m^{-2}$. (B)-(E) show the relationship between observed top-of-canopy leaf traits and their light plasticity coefficients. A solid line indicates a significant linear relationship ($p < 0.05$), whereas a dashed line indicates an insignificant relationship. Green lines and numbers indicate the regression results fitted without outlier (leaf dark respiration > 2 μmol $m^{-2}\ s^{-1}$ or specific leaf area > 20 $m^2\ kg^{-1}$).

2.5 PFT definition and parameterization

Tropical tree species are commonly classified into PFTs based on plant physiological traits, particularly wood density, because these traits are associated with a species' position on a growth-mortality tradeoff axis (Wright et al., 2010). However, 35% of all inventoried species at the BCI plot do not have wood density information, and only 8% of all species have local measurements for all leaf traits of interest (leaf dark respiration rate, V_{cmax}, SLA, and leaf lifespan), thus a trait-based PFT definition is limited by data availability. To overcome this data limitation, we developed a metric named demographic niche score to define PFTs based on demography rather than physiological traits, following previous practices to classify tropical species using demographic rates (Condit & Rüger, 2022; Rüger et al., 2020).

First, we grouped all inventoried individuals into 20-meter patches based on their spatial locations and calculated oLAI for each individual within each patch. oLAI values were calculated from a DBH-based leaf area allometric function as described in section 2.3. Second, for each species, we calculated the relative DBH growth rate of individuals under high light (the smallest 25% oLAI) and the mortality rate of individuals under low light (the largest 25% oLAI). Third, we performed principal component analysis (PCA) for the species-level high light growth rates and low light mortality rates (both were log transformed before the PCA analysis). We used the first principal component as the demographic niche score, which explained 71% of the total variation in demographic rates (**Fig. S1**).

Standard major axis regression revealed a strong positive relationship between species-level demographic niche score and wood density (**Fig. S2A**), implying that our demographic niche score can reasonably represent species' position on the growth-mortality tradeoff axis.

In ED2-baseline and ED2-plastic, there are three PFTs: early-successional (species with lowest 33% demographic niche score), late-successional (species with top 33% demographic niche score), and mid-successional (intermediate score). From 1990-2010, the BCI plot on average has 6.65, 9.40, and 15.1 $cm^2\ m^{-2}$ (measured by basal area) of early-, mid- and late-successional PFT. To parameterize top-of-canopy leaf trait values ($\boldsymbol{X_{i,0}}$ in equation 2) for these three PFTs, we performed standardized major axis regression between species-level demographic niche score and top-of-canopy V_{cmax} at 25°C, SLA, and leaf lifespan in W03 dataset

(**Fig. S2**), then we parameterized $\boldsymbol{X_{i,0}}$ based on the median demographic niche score of each PFT. Based on the regression models, early-successional PFT has the highest top-of-canopy V_{cmax}, largest SLA, and shortest leaf lifespan. For $\boldsymbol{Respiration_{i,0}}$, we parameterized it to be proportional to $\boldsymbol{V_{cmax\,i,0}}$ by a factor of 0.015. When oLAI > 0, the simulated respiration to V_{cmax} ratio will deviate from 0.015 because leaf dark respiration is more plastic than V_{cmax} (**Table S1**), resulting in a lower ratio with increasing oLAI (**Fig. S3E**).

The three PFTs described above are parameterized by top-of-canopy leaf trait values. For ED2-static, we defined an additional 15 PFTs which are parameterized by understory leaf trait values. Specifically, for each of the three original PFTs, we calculated leaf dark respiration at 25°C, V_{cmax} at 25°C, SLA, and leaf lifespan values at oLAI of 1, 2, 3, 4, 5 $m^2\ m^{-2}$ based on equation 2, then we generated five new PFTs by assigning these leaf trait values as new $\boldsymbol{X_{i,0}}$ and keeping all other traits (e.g., wood density, mortality parameters) the same as the original PFT. In total, ED2-static includes six early-successional PFTs, six mid-successional PFTs, and six late-successional PFTs. The variation in $\boldsymbol{X_{i,0}}$ across these 18 PFTs is identical to the plasticity-driven variation in $\boldsymbol{X_{i,j,new}}$ across an oLAI gradient of 0-5 $m^2\ m^{-2}$.

2.6 Simulation protocol

To test our first two hypotheses, we initialized the model with the BCI forest census in 1990, ran the model from 1989 to 2010 (hereafter short-term simulation), and compared demographic rates and forest structure simulated by ED2-baseline, ED2-plastic, and ED2-static. Since we were interested in the dynamics of tree species, we excluded herbaceous species and only used the census information of woody species in the initialization. To test the third and fourth hypotheses, we simulated 300-year forest secondary succession from a near bare-ground condition (hereafter long-term simulation), and compared the forest composition and functioning simulated by the three models. A near bare-ground condition means that there are only a few tree seedlings of each PFT at the start of the simulation. The forest was simulated for 300 years because total basal area and aboveground biomass reached steady state during this time frame. We used an *in situ* climate dataset collected at BCI from 1985-2012 as meteorological forcing (available through the Smithsonian Tropical Research Institutes' Physical

379 Monitoring Program), and all simulations used repeated cycles of this multi-year climate
380 dataset. The long-term simulations used a disturbance rate of 0.014 $year^{-1}$, which is the default
381 value in ED2 (Moorcroft et al., 2001).

382 2.7 Model benchmarking and analysis

383 To evaluate the prediction of demographic rates and forest structure, we calculated the
384 simulated growth rate, mortality rate, plant density, and leaf area averaged during 1990-2010
385 in short-term simulations, then compared it to observations. Specifically, we calculated
386 observed annual DBH growth rates and mortality rates for every two BCI censuses and then
387 calculated average demographic rates during 1990-2010. We didn't use census data earlier than
388 1990, since DBH values smaller than 5.5 cm were rounded down to the nearest 5 mm in earlier
389 censuses. In terms of forest structure, we calculated the size distribution of plant density
390 averaged during 1990-2010. We also used a leaf area vertical profile estimated by airborne
391 LiDAR (Detto et al., 2015) as a model benchmark.

392 To measure the simulated tree shade tolerance, we calculated the PFT-level growth
393 compensation point (GCP), defined as the oLAI at which DBH growth rate declines to 0.01 cm
394 $year^{-1}$ (**Fig. 3A**). A higher GCP value suggests a higher shade tolerance. The community-level
395 GCP is calculated using all cohorts across all PFTs with DBH ≥ 1 cm.

396 To evaluate the prediction of long-term forest functioning, we calculated the plant
397 density, basal area, LAI, and gross primary productivity (GPP) averaged across the last 20 years
398 of long-term simulations. We also compared the simulated aboveground biomass (AGB)
399 trajectories with two sets of field-based AGB estimates: one is AGB estimates across a 300-year
400 chronosequence in Panama (Batterman et al., 2013), and the other is a BCI plot-level estimate
401 calculated based on the 2010 census and a local height allometry (Cano et al., 2019). Besides,
402 we compared simulated GPP to flux tower-based GPP measurements at BCI (Detto & Pacala,
403 2022).

404 To evaluate the prediction of trait diversity, we calculated a metric named community-
405 level vertical trait gradient for both observations and simulations. Using ten vertical leaf trait

406 profiles measured in Panama, Lamour et al. (2023) fitted power law equations between
407 observed trait values (pooled across multiple species) and oLAI. The fitted scaling exponent
408 (reported in Table S3 and S4 of Lamour et al. 2023) represents the observed community-level
409 vertical trait gradient, which is the result of both intra-specific light plasticity and vertical
410 stratification of species composition. We similarly calculated the modeled community-level
411 vertical trait gradient by fitting a power law equation between cohort-level trait values and
412 modeled oLAI.

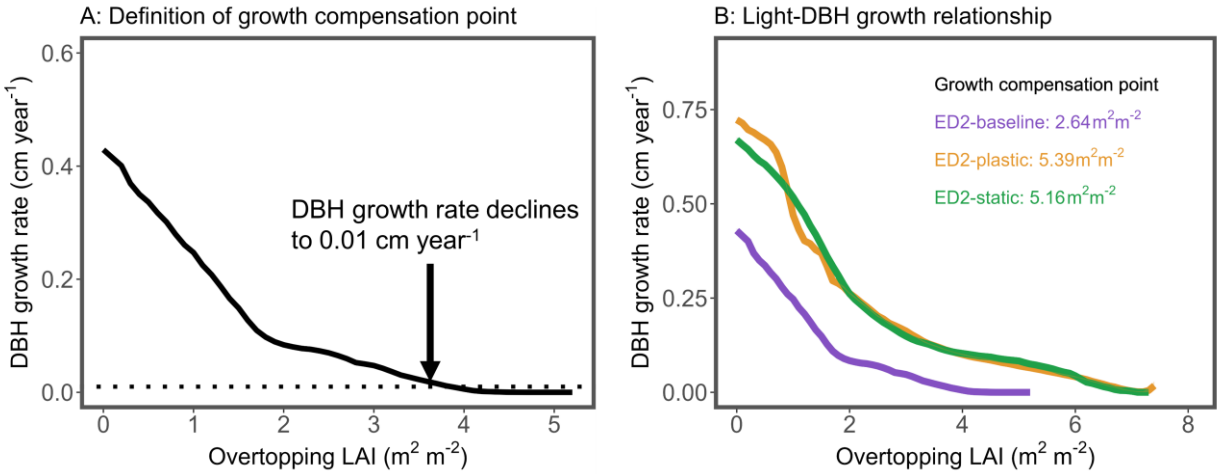

413 **Figure 3**. The definition of growth compensation point and the simulated relationship between
414 DBH growth rate and overtopping LAI. (A) shows a conceptual diagram of how growth
415 compensation point (GCP) is defined. GCP is a measure of simulated shade tolerance, and it is
416 calculated as the overtopping LAI at which modeled DBH growth rate declines to 0.01 cm year^{-1}
417 (represented by the dotted line), and a larger GCP indicates a higher shade tolerance. (B)
418 Simulated relationships between DBH growth rate and overtopping LAI for all DBH ≥ 1 cm
419 cohorts during short-term simulations. ED2-baseline, ED2-plastic, and ED2-static are
420 represented by purple, orange, and green lines, respectively. Inserted texts report simulated
421 GCP for each model.

422

423 **3 Results**

424 3.1 Tree demographic rates in short-term simulations

425 We compared 20-year-average growth rates predicted by ED2-baseline and ED2-plastic
426 in short-term simulations with the census data. In ED2-baseline, the DBH growth rate of

understory cohorts (DBH: 1-10cm) was 0.0429 cm year^{-1}, and incorporating observation-constrained light plasticity in ED2-plastic increased simulated understory growth rate to 0.0865 cm year^{-1}, closer to the observed 0.0723 cm year^{-1} (**Fig. 4A**). At the PFT level, ED2-baseline predicted understory growth to be 0.0107, 0.00447, and 0.0456 cm year^{-1} for early-, mid-, and late-successional PFTs, lower than the observed growth rates of 0.203, 0.0637, and 0.0679 cm year^{-1} (**Fig. 4B**). Light plasticity improved model-data agreement by increasing the PFT-level understory growth to 0.145, 0.0878, and 0.0847 cm year^{-1}. This increase was substantially larger in early- and mid-successional PFT than in late-successional PFT (1255% and 1864% compared to 85.7%).

We also tested the growth effect of increasing inter-specific diversity. The average understory growth rate simulated by ED2-static was 0.0949 cm year^{-1}, which more than doubled the estimate of ED2-baseline and better aligned with the observation (**Fig. 4A**). At the PFT level, simulated growth rates were 0.104, 0.0415, and 0.111 cm year^{-1} for early-, mid-, and late-successional PFT, and these PFT-level estimates were higher than ED2-baseline and comparable to ED2-plastic (**Fig. 4B**).

Although both light plasticity and inter-specific diversity improved model-data agreement of understory growth rates, only ED2-plastic correctly predicted that the understory growth rate of early-successional PFT was highest among all PFTs (**Fig. 4B**), whereas ED2-baseline and ED2-static wrongly predicted late-successional PFT to have the fastest growth.

The understory mortality rate simulated by ED2-baseline was 126% higher than the census observation (0.0531 year^{-1} compared to 0.0235 year^{-1}). ED2-plastic and ED2-static reduced the model overestimate to 0.0380 and 0.0388 year^{-1}, respectively (**Fig. 5**).

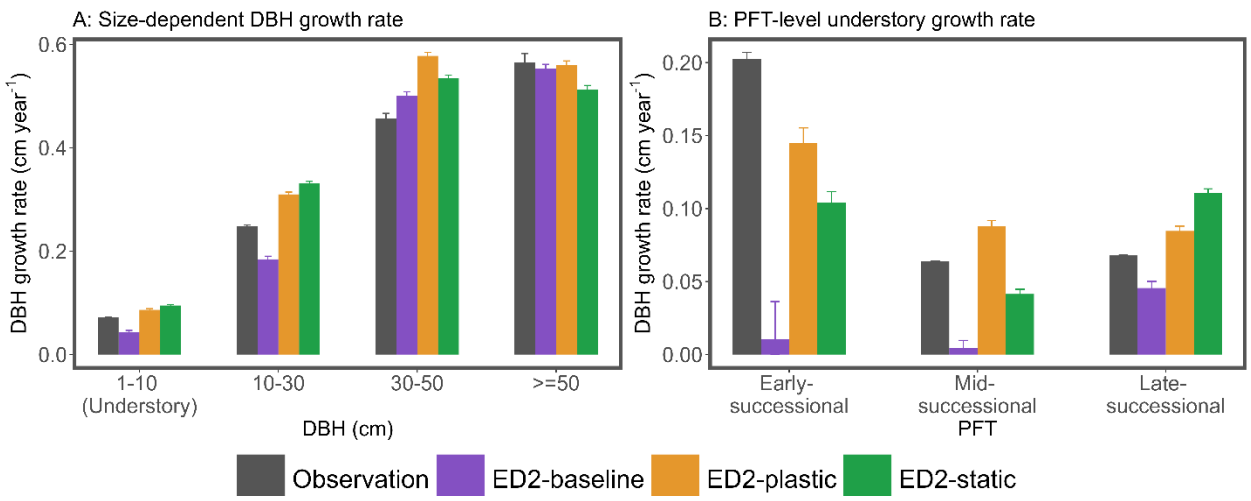

Figure 4. Light plasticity effect on 20-year-average tree growth during short-term simulations. (A) shows modeled and observed DBH growth rates for different size classes. ED2-baseline, ED2-plastic, and ED2-static are represented by purple, orange, and green bars, respectively. (B) shows modeled and observed understory DBH growth rates for different PFTs. Understory is defined as trees or cohorts with DBH between 1-10 cm. Error bars indicate 95% confidence intervals calculated by bootstrapping.

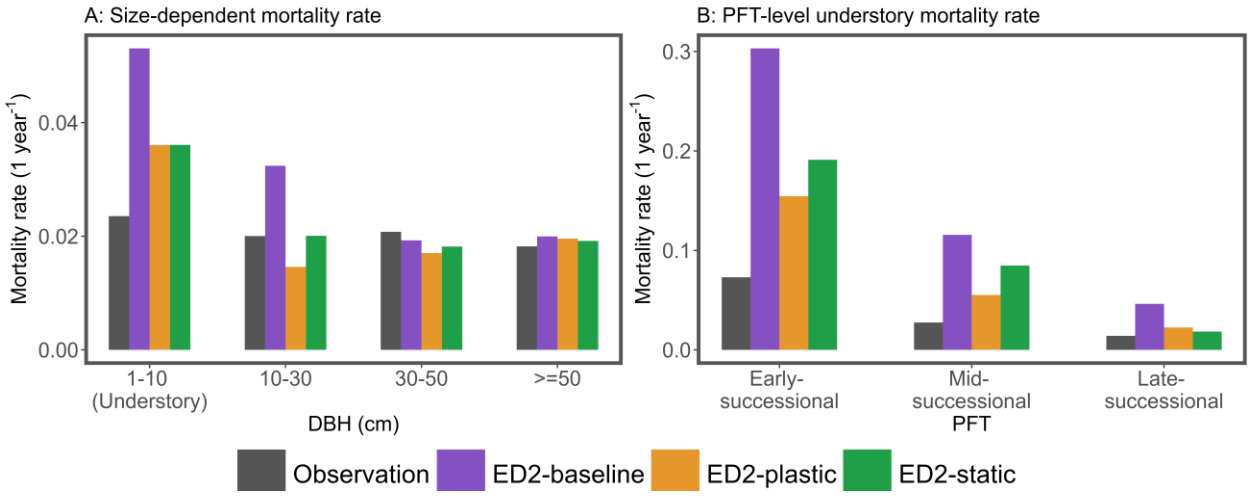

Figure 5. Light plasticity effect on 20-year-average mortality rate during short-term simulations. (A) shows modeled and observed mortality rates for different size classes. ED2-baseline, ED2-plastic, and ED2-static are represented by purple, orange, and green bars, respectively. (B) shows modeled and observed understory mortality rates for different PFTs. Understory is defined as trees or cohorts with DBH between 1-10 cm.

3.2 Forest structure in short-term simulations

We analyzed the 20-year-average size distribution of plant density and leaf area profile in the short-term simulations. Simulated understory plant density in ED2-baseline was 0.0931 plant m^{-2}, and light plasticity increased community-level understory plant density to 0.260 plant m^{-2}, bringing it closer to the observed 0.391 plant m^{-2} (**Fig. 6A**). At the PFT level, the understory plant density of early-, mid-, and late-successional PFT were 0.00106, 0.0110, and 0.0847 plant m^{-2} in ED2-baseline, which were an order of magnitude lower than the observed 0.0272, 0.161, and 0.203 plant m^{-2}. Light plasticity increased plant densities to 0.00301, 0.0972, and 0.159 plant m^{-2}, reducing the underestimates (**Fig. 6B**). The increase in mid-successional PFT abundance contributed the most to the improved model-data agreement of community-level understory plant density.

ED2-static increased community-level understory plant density to a more realistic 0.217 m^{-2}, accompanied by 86.9-252% PFT-level increases relative to ED2-baseline. Community- and PFT-level understory plant density predictions were comparable between ED2-static and ED2-plastic (**Fig. 6**).

Underestimates of plant density in ED2-baseline further led to underestimated leaf area in the understory (**Fig. 6C**). Meanwhile, the leaf area vertical profile simulated by ED2-plastic and ED2-static aligned with an airborne LiDAR-based estimate (Detto et al., 2015). The total LAI predicted by ED2-plastic and ED2-static (5.86 and 5.24 $m^2\ m^{-2}$) was higher than ED2-baseline prediction of 3.11 $m^2\ m^{-2}$, and ED2-plastic estimate best aligned with a total LAI estimate of 5.9 ± 0.4 $m^2\ m^{-2}$ based on hemispherical photos (Detto et al., 2018).

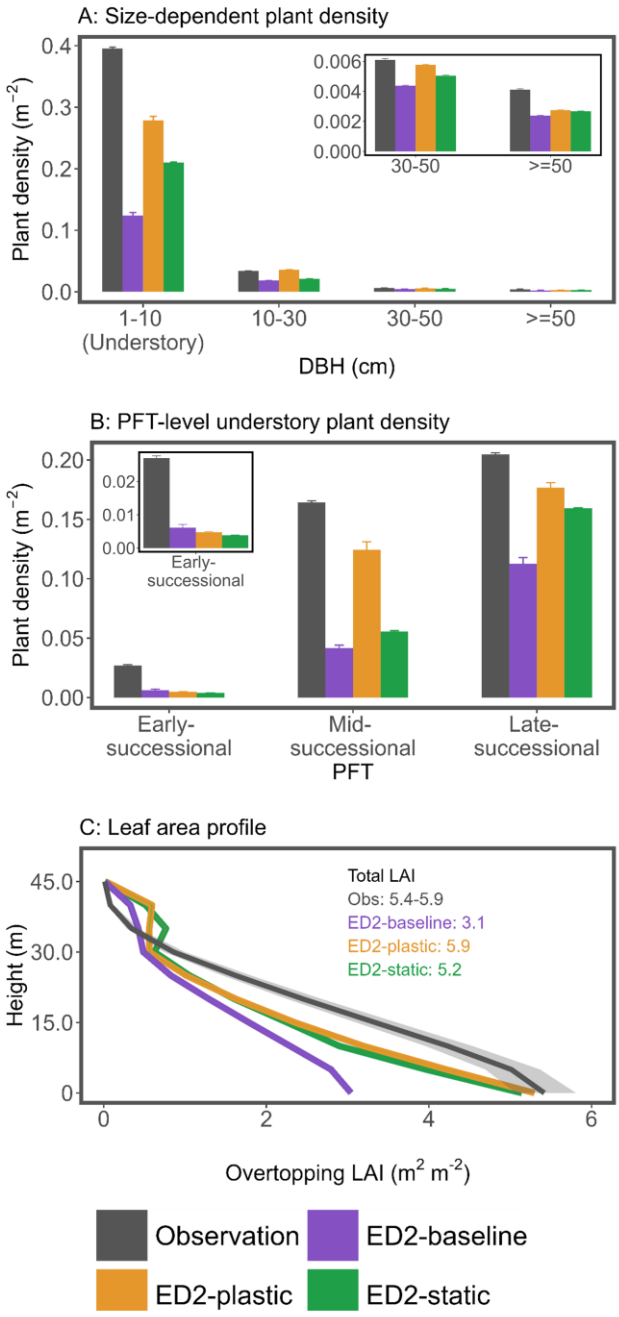

Figure 6. Light plasticity effect on 20-year-average forest structure during short-term simulations. (A) shows modeled and observed plant density for different size classes. ED2-baseline, ED2-plastic, and ED2-static are represented by purple, orange, and green bars, respectively. The inset figure is an enlarged version of the modeled and observed plant density for cohorts with DBH ≥ 30 cm. Error bars indicate 95% confidence intervals calculated by bootstrapping. (B) shows modeled and observed understory plant density for different PFTs. The inset figure is an enlarged version of the modeled and observed plant density for early-successional PFT. Error bars indicate 95% confidence intervals calculated by bootstrapping. (C)

514 shows the vertical profile of overtopping LAI. Inserted texts report the observed and modeled
515 total LAI. Airborne-LiDAR based estimate is 5.4 m^2 m^{-2} (Detto et al., 2015), and hemispherical
516 photo-based estimate is 5.9 m^2 m^{-2} (Detto et al., 2018). Gray shaded area indicates 95%
517 confidence interval of the LiDAR-based estimate.

518

519 3.3 Forest dynamics in long-term simulations

520 We examined AGB, GPP, PFT composition, and trait composition during simulations of
521 300-year forest secondary succession. At the 12th and 80th years of succession, the forest
522 simulated by ED2-baseline stored 32.4 and 123 Mg ha^{-1} of AGB, lower than chronosequence-
523 based estimates of 88.0 and 160 Mg ha^{-1} (Batterman et al., 2013), and ED2-plastic generated
524 higher and more realistic estimates of 50.7 and 175 Mg ha^{-1} (**Fig. 7A; Table 2**). At the 300th year,
525 ED2-plastic predicted AGB to be 224 Mg ha^{-1} (**Table 2**), which was 50.3% higher than ED2-
526 baseline estimate, though still lower than the census-based estimate of 263-266 Mg ha^{-1} (Cano
527 et al., 2019). ED2-static predicted total AGB to be 57.5, 154, and 233 Mg ha^{-1} after 12, 80, and
528 300 years of succession, which were similar to or higher than the predictions with light
529 plasticity.

530 During the last 20 years of succession, ED2-plastic produced the highest GPP estimate of
531 3.39 kg C m^{-2} $year^{-1}$, whereas ED2-static predicted the lowest GPP of 2.23 kg C m^{-2} $year^{-1}$. The
532 prediction of ED2-baseline (2.83 kg C m^{-2} $year^{-1}$) best aligned with the observed value of 2.8 kg
533 C m^{-2} $year^{-1}$ (Detto & Pacala, 2022).

534 All models exhibited a similar temporal trend of community composition, where early-
535 successional PFT initially dominated the forest and was eventually outcompeted by late-
536 successional PFT (**Fig. 8**). During the last 20 years of succession, all models underestimated the
537 basal area of early-successional PFT relative to the abundance observed in BCI forest censuses
538 (**Fig. 7B**), but the ED2-plastic estimate of 3.07 cm^2 m^{-2} best aligned with the observed 6.65 cm^2
539 m^{-2}, whereas ED2-baseline and ED2-static underestimated the basal area by an order of
540 magnitude (0.417 and 0.618 cm^2 m^{-2}).

541

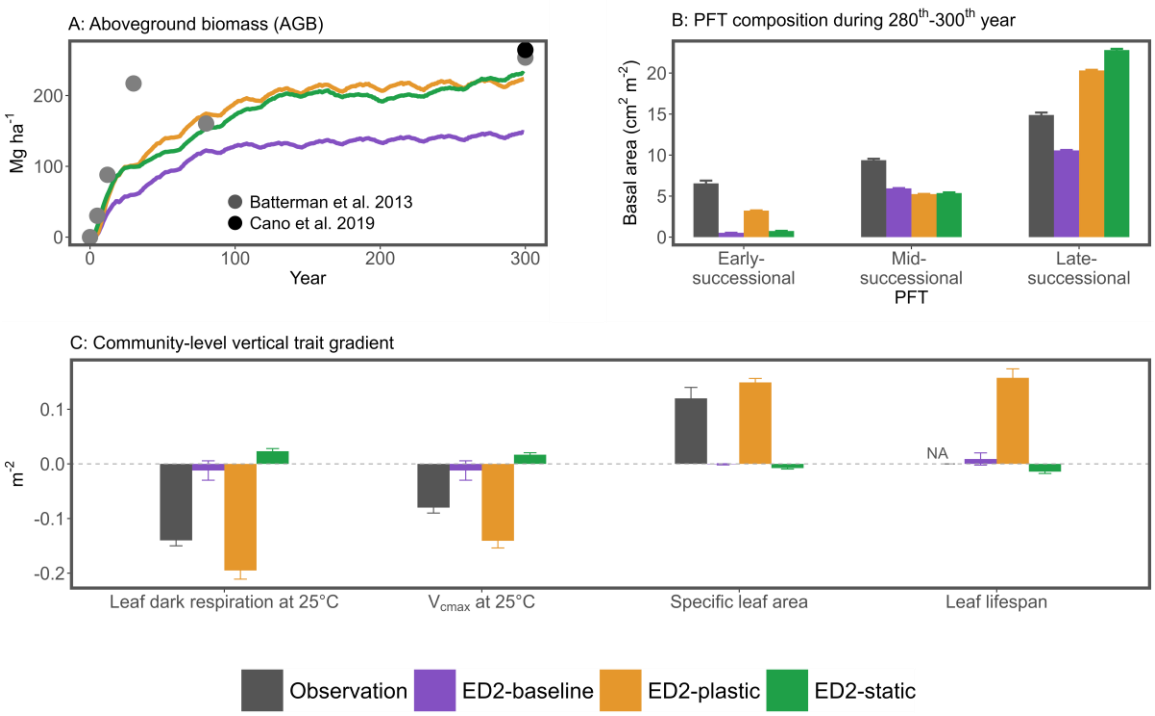

Figure 7. Light plasticity effect on 300-year forest secondary succession in long-term simulations. (A) shows the trajectory of aboveground biomass (AGB) modeled by ED2-baseline (purple line), ED2-plastic (orange line), and ED2-static (green line). Gray points represent observations from a chronosequence in Panama (Batterman et al., 2013). The black point represents the plot-level AGB estimate based on censuses and local allometric equations (Cano et al., 2019). (B) shows the simulated and modeled PFT abundance averaged during the last 20 years of succession. (C) shows modeled and observed community-level vertical trait gradients of leaf dark respiration rate at 25°C, V_{cmax} at 25°C, specific leaf area, and leaf lifespan. The definition and calculation of community-level vertical trait gradient are described in section 2.7. ED2-baseline, ED2-plastic, and ED2-static are represented by purple, orange, and green bars, respectively. Error bars for these simulated results are 95% confidence intervals calculated by bootstrapping. Gray bars and gray error bars represent the observed community-level vertical trait gradients and their confidence intervals reported in Table S3 and S4 in Lamour et al. (2023). The observed leaf lifespan gradient is marked as "NA" because Lamour et al. (2023) did not collect leaf lifespan data.

The simulated community-level trait diversity also differed across models. In ED2-plastic, the community-level vertical trait gradient (defined in section 2.7) of leaf dark respiration, Vcmax, and SLA were -0.195, -0.141, and 0.149, which were comparable to the -0.14, -0.08, and 0.12 reported in Lamour et al. (2023) based on in situ trait measurements (**Fig. 7C**). In contrast, both ED2-baseline and ED2-static showed vertical trait gradients that were close to zero, i.e.,

582 leaf dark respiration, Vcmax, and SLA were largely constant within the canopy. Aside from trait
583 profiles, community-average leaf traits (weighted by cohort-level leaf area) during the last 20
584 years of succession were also different between models. Average leaf dark respiration and
585 Vcmax were 104% and 64.1% higher in ED2-plastic than in ED2-static, while SLA, leaf lifespan,
586 and wood density were 40.3%, 50.6%, 3.72% higher in ED2-static than in ED2-plastic (Table 2).
587

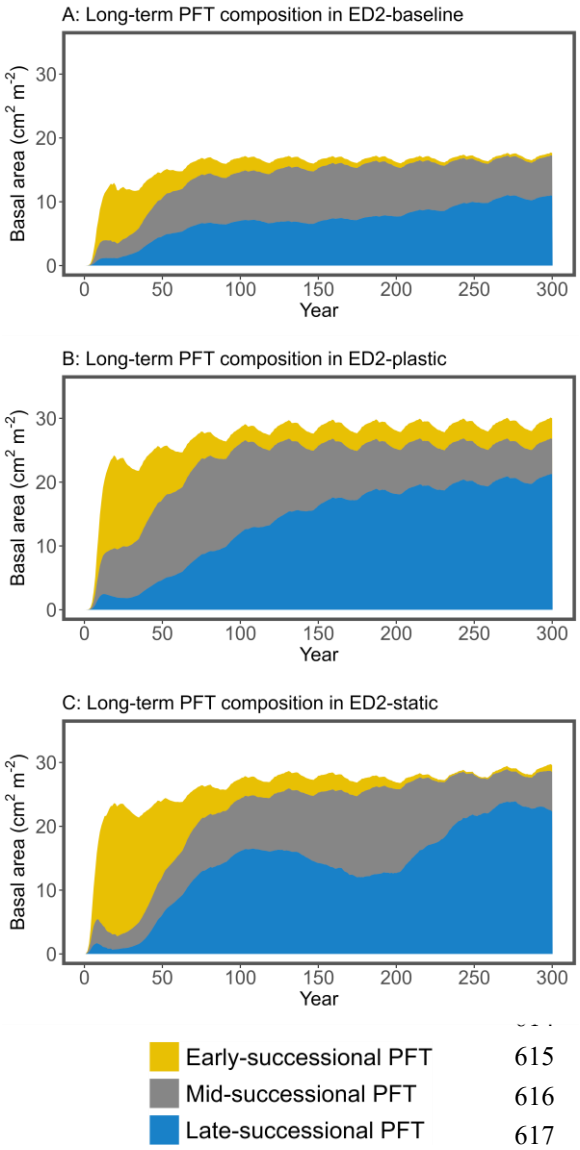

618
619 **Figure 8**. Light plasticity effect on community composition in long-term simulations. (A)-(C)
620 show PFT composition in ED2-baseline, ED2-plastic, and ED2-static. Early-, mid, and late-
621 successional PFTs are shown in yellow, gray, and blue areas, respectively.
622

Table 2. Modeled forest structure, composition, trait diversity, and functioning in long-term simulations. Trait values are calculated as community-level averages weighted by cohort-level leaf area during the last 20 years of simulation. All other variables are calculated as ecosystem-level averages during the last 20 years of simulation, except for AGB. AGB is an annual average. For example, AGB at the 12th year is calculated as the ecosystem-level, annual average during the 12th year of the simulation.

	ED2-baseline	ED2-plastic	ED2-static	Observation
Forest structure and composition				
Total plant density (individuals m^{-2})	0.206	0.424	0.367	0.433 (forest census)
Understory plant density (individuals m^{-2})	0.181	0.378	0.325	0.391 (forest census)
Total basal area (cm^2 m^{-2})	16.9	28.7	28.7	30.7 (forest census)
Total LAI (m^2 m^{-2})	3.16	6.25	5.81	5.42 (Detto et al., 2018); 5.9 (Detto et al., 2015)
Basal area of early-successional PFT (cm^2 m^{-2})	0.417	3.07	0.618	6.65 (forest census)
Community-level trait diversity				
Leaf dark respiration rate at 25°C (μmol m^{-2} s^{-1})	0.760	0.417	0.204	NA
V_{cmax} at 25°C (μmol m^{-2} s^{-1})	50.7	32.5	19.8	NA
Specific leaf area (m^2 kg^{-1})	11.2	21.6	30.3	NA
Leaf lifespan (month)	12.0	26.9	40.5	NA
Wood density (g cm^{-3})	0.622	0.619	0.642	NA

Forest functioning				
AGB at 12th year (Mg ha^{-1})	32.4	50.7	57.5	88.0 (Batterman et al., 2013)
AGB at 80th year (Mg ha^{-1})	123	175	154	160 (Batterman et al., 2013)
AGB at 300th year (Mg ha^{-1})	149	224	233	263-266 (Cano et al., 2019)
Gross primary productivity (kg C m^{-2} year^{-1})	2.85	3.39	2.23	2.8 (Detto & Pacala, 2022)

4 Discussion

4.1 Light plasticity and inter-specific diversity similarly correct for model biases in understory growth and forest structure

Consistent with our first hypothesis, growth rates of understory trees were underestimated by 40.7% when they were not plastic and were parameterized by top-of-canopy leaf traits (**Fig. 4A**). Incorporating observation-based light plasticity corrected for this growth underestimate and further enabled accurate prediction of tree size distribution and leaf area profile (**Fig. 4 and 6**), which supports our second hypothesis. These findings provide the first quantitative evidence that light plasticity is critical for explaining demographic processes and forest structure, and that observation-constrained light plasticity largely corrects for the model underestimate of understory growth and abundance in tropical forests.

The modeled effects of light plasticity arise from increased plant shade tolerance. The simulated community-level GCP doubled with light plasticity (**Fig. 3B**), with the largest increase in early-successional PFT (**Fig. S4**). Field experiments have similarly shown that plants in low light treatment substantially reduce their light compensation point (LCP; a lower LCP suggests a higher shade tolerance) compared to conspecifics in high light treatment. For example, Kitajima

(1994) showed that tropical tree seedlings grown in the shaded treatment can reduce their leaf-level LCP by more than 50% compared to conspecifics grown in the full sun. Sterck et al. (2013) showed that the plant-level LCP of tropical tree seedlings grown at the low light level decreased to one-third of conspecifics grown at the high light level. The magnitude of increase in shade tolerance is comparable between field observations and our modeling results, suggesting that the simulated physiological consequences of light plasticity are realistic.

Meanwhile, ED2-static with higher inter-specific diversity predicted similar understory growth and forest structure as ED2-plastic during short-term simulations (**Fig. 4 and 6**). Although ED2-static did not incorporate light plasticity, it generated within-canopy trait profiles and GCPs that were similar to ED2-plastic (**Fig. S3 and S4**) by including additional PFTs. Therefore, incorporating within-canopy variation in leaf traits, either by including intra-specific light plasticity or expanding inter-specific diversity, is necessary to predict realistic understory growth and tropical forest structure.

This finding is relevant to recent efforts to improve the representation of fine-scale functional diversity in TBMs. For example, hyperspectral imaging has been used to initialize PFT composition at a high spatial resolution (Bogan et al., 2019). Although this approach captures spatial heterogeneity in plant functional traits, it does not explicitly account for the within-canopy trait variation. Our results emphasize that a TBM only including the trait variation observed at the top canopy (such as ED2-baseline) is insufficient for predicting tropical forest structure, instead, such prediction requires incorporating the within-canopy trait diversity. Future research should extend beyond our plot-level findings to quantify the ecological consequences of within-canopy trait diversity at a larger spatial scale and across different tropical regions.

4.2 Light plasticity effect on long-term functional composition and within-canopy trait profiles cannot be compensated by inter-specific diversity

The demographic effects of light plasticity and inter-specific diversity further modulate long-term forest succession and regrowth. We found that ED2-plastic and ED2-static similarly

673 enhanced modeled biomass accumulation relative to ED2-baseline during 300 years of
674 succession (**Table 2; Fig. 7A**), supporting our third hypothesis but not the fourth hypothesis.

675 Despite the positive effects of light plasticity and inter-specific diversity, AGB predictions
676 at the 300th year across all models were still lower than the plot-level estimate based on local
677 allometry (Cano et al., 2019). This is attributed to an underestimate of large tree growth and an
678 overestimate in their mortality rates (**Fig. 4A and 5A**), which may be related to the inaccurate
679 representation of size dependence in reproductive allocation and aboveground versus
680 belowground allocation (Xu et al., 2024).

681 Although ED2-plastic and ED2-static generated similar predictions of AGB, the effect of
682 light plasticity on improving the prediction of functional composition cannot be compensated
683 by inter-specific diversity. Early-successional PFT was largely outcompeted by mid- and late-
684 successional PFTs in ED2-static, whereas it coexisted with other PFTs at a substantially higher
685 abundance in ED2-plastic (**Table 2**). This difference arises because inter-specific diversity and
686 light plasticity shape community assembly differently. In ED2-static, light limitation imposes a
687 strong selection pressure on understory trees, particularly for early-successional PFTs. In
688 contrast, intra-PFT plasticity enhances individual fitness, especially the fitness of early-
689 successional PFT which is the most plastic (**Table S1**), eventually promoting coexistence.

690 The unique effect of light plasticity on composition is also evident at the trait level.
691 During long-term simulations, ED2-plastic generated a realistic community-level vertical trait
692 gradient (defined in section 2.7), whereas leaf traits simulated by ED2-static did not vary
693 significantly across the vertical gradient (**Fig. 7C**). This is because in ED2-static, only trees with
694 shade-tolerant traits can survive the understory stage and then reach the top canopy, thus ED2-
695 static simulated values of leaf dark respiration rate and V_{cmax} were always low, and values of
696 SLA and leaf lifespan were always high, regardless of the canopy position (**Fig. S5**). In contrast,
697 trees in ED2-plastic dynamically adjust their traits based on light levels throughout their
698 lifetime. As a result, ED2-static had 51.1% and 39.1% lower community-level leaf dark
699 respiration and V_{cmax} than ED2-plastic, further leading to a 34.2% lower GPP (**Table 2**). The

community-average leaf dark respiration and V_{cmax} were the highest in ED2-baseline because all cohorts in this model had top-of-canopy trait values.

Interestingly, GPP simulated by ED2-baseline best aligned with the flux tower-based estimate during 2012-2017 (Detto & Pacala, 2022). This model-data agreement in GPP does not arise from an accurate representation of ecophysiological processes, rather, it arises from the compensatory effect of an underestimated LAI and a high V_{cmax}. Meanwhile, ED2-plastic predicted realistic trait profiles and LAI, but overestimated GPP by 21.1%. This may be explained by a lack of hydraulic limitation (Xu et al., 2016) in the version of ED2 used for our study and possible biases in stomatal parameters and photosynthetic temperature dependence.

Results of PFT composition and community-level trait diversity suggest that light plasticity regulates tropical forest functional composition differently from inter-specific trait variation, and this finding sheds new light on how we should represent functional diversity in trait-based modeling. Higher simulated functional diversity have been shown to improve the prediction of ecosystem carbon fluxes and biomass resilience, and this higher diversity is often achieved by increasing the number of PFTs (Butler et al., 2022; Pappas et al., 2016; Pavlick et al., 2013; Rius et al., 2023; Sakschewski et al., 2016). Extending beyond these findings, we show that increasing the inter-PFT diversity is not sufficient for predicting long-term forest dynamics, and the intra-PFT trait variation across microenvironmental gradients is required for realistic prediction of forest functional composition.

Based on the demonstrated role of light plasticity in demography, forest structure, and composition, we further hypothesize that light plasticity will regulate ecosystem responses to light environment variability, particularly gap formations and post-disturbance forest regeneration. First, light plasticity maintains the abundance of light-demanding species prior to gap formation and thus facilitates future gap colonization and regrowth of these species. Second, light plasticity will increase the photosynthesis and growth of previously suppressed understory trees after gap formation by trait adjustment to elevated light levels. These hypotheses, although yet to be tested, are particularly relevant for mechanistic understanding

728 of tropical secondary forests, which now occupy more than half of all tropical forests (Food and
729 Agriculture Organization of the United Nations, 2010) and are predicted to have large regrowth
730 potential (Anderson-Teixeira et al., 2016; Pan et al., 2011; Pugh et al., 2019; Shevliakova et al.,
731 2009). Future research should investigate the role of light plasticity in predicting the multi-
732 dimensional recovery of tropical secondary forests (Poorter *et al.*, 2021).

733 4.3 Toward mechanistic modeling of trait plasticity

734 By incorporating the variation in light plasticity across different species and traits, our
735 study provides a more realistic representation of light plasticity than previous TBMs (**Table 1**).
736 However, our representation of light plasticity has several assumptions about the degree,
737 timescale, and ecological consequences of trait plasticity. These assumptions, which have not
738 been thoroughly evaluated, highlight the key challenges and opportunities for further
739 developing a more mechanistic characteriziation of trait plasticity in TBMs.

740 We assumed that intra-specific light plasticity is the only driver of observed within-
741 canopy trait gradient, which may lead to an overestimate of the degree of light plasticity. While
742 light is a primary cue of the vertical variation, ontogeny can also contribute significantly to leaf
743 trait plasticity, particularly for non-pioneer species (Wen et al., 2008). In addition, thermal
744 stress, water stress, and herbivory can all contribute to the vertical trait profile (Cavaleri et al.,
745 2010; Coste et al., 2009; Dang-Le et al., 2013). Field-based trait measurements across a wider
746 range of ontogenetic stages and microenvironmental gradients will be instrumental in
747 disentangling the contribution of trait plasticity from these other sources of variation.

748 Another key assumption is that light plasticity only occurs at the time of leaf turnover
749 and that traits remain constant within a leaf's lifetime, and such assumption may have
750 underestimated the rate of plasticity adjustment. Results from warming experiments have
751 shown that the timescale of temperature acclimation in leaf dark respiration varies from two
752 weeks to two months (Reich et al., 2021; Ren et al., 2024), and a similar analysis is yet to be
753 conducted to determine the timescale of plasticity-induced trait adjustments driven by other
754 environmental factors.

Our results emphasized the benefits of light plasticity, but phenotypic plasticity is not necessarily adaptive. For example, the expression of plasticity can be energetically costly, and plasticity may lower fitness under certain scenarios (DeWitt et al., 1998). We did not model these processes because field-based quantitative assessments are rare, and the few studies did not find consistent evidence for the costs and tradeoffs associated with plasticity (Avramov et al., 2007; McIntyre & Strauss, 2014; Liu et al., 2016). On the other hand, TBM can serve as a useful tool to quantify the cost of plasticity. For example, the metabolic cost of trait plasticity can be incorporated as a model parameter, and optimizing the parameter against observed forest demography and carbon fluxes may serve as a first-order estimate of the cost.

While we focused on the light-driven plasticity of leaf physiological traits in this study, trait plasticity is a widespread phenomenon observed in other traits and across other environmental gradients (Poorter et al., 2019; Siefert et al., 2015). For example, plant structural traits such as leaf angle vary substantially within the canopy, which can influence carbon and energy fluxes (Yang et al., 2023). In addition to leaf traits, plant allometry and root traits are also known to be plastic (Poorter et al., 2019; Yaffar et al., 2024). A mechanistic understanding and representation of trait plasticity is thus a research frontier in vegetation modeling, and it will ultimately benefit from field-based trait sampling accompanied by comprehensive measurements of the microenvironment. Recent years have already seen increasing field campaigns that measure plant morphological and physiological traits across different microenvironments (Lamour et al., 2023; Poorter et al., 2018). These datasets attempt to characterize the variation of both functional traits and environmental factors at a scale that is ecologically relevant to individual plant performance, and they will provide useful information for both quantitative characterization of trait plasticity and its incorporation in trait-based models.

5 Conclusions

781 Plant functional diversity in traits associated with light use, including both inter-specific
782 and intra-specific variation, critically shapes tropical forest dynamics by modulating tree
783 demography. By combining trait measurements, long-term census data, and trait-based
784 ecosystem modeling, we showed that observation-constrained light plasticity enhances
785 understory growth and abundance. This demographic effect further increases long-term
786 tropical forest biomass accumulation and strongly modulates forest structure and composition.
787 Importantly, the community and ecosystem effects of light plasticity cannot be fully
788 compensated by increasing inter-specific functional diversity, particularly in terms of
789 community composition and within-canopy trait gradients. These findings suggest that light
790 plasticity is crucial for trait-based prediction of tropical forest regrowth and resilience,
791 especially in secondary forests which experience high variability and heterogeneity in the light
792 environment. Future research should quantify phenotypic plasticity across a broader range of
793 traits and environmental gradients and evaluate their community and ecosystem-level impact.

794

795 **Acknowledgments**

796 XX and YM were supported by DOE Environmental System Science Program grant DE-
797 SC0023048 and NSF grant 2140581. AR, JL, KD, and SS were supported by the Next Generation
798 Ecosystem Experiments-Tropics project funded by the US Department of Energy, Office of
799 Science, Office of Biological and Environmental Research, and by U.S. Department of Energy
800 Contract No. DE-SC0012704 to Brookhaven National Laboratory. AR was also supported by U.S.
801 Department of Energy Contract No. DE-AC02-05CH11231 to Lawrence Berkeley National
802 Laboratory. SS was also supported by the NASA Surface Biology and Geology Mission. MD was
803 supported by the Carbon Mitigation Initiative at Princeton University and NSF grant 2017804.

804 The authors declare no conflict of interest.

805

806 **Open Research**

807 Census data used for model benchmarking are publicly available at
808 https://datadryad.org/stash/dataset/doi:10.15146/5xcp-0d46. Previously published trait data is

described in Lamour et al. (2023). All scripts for ED2 model simulations are available at https://github.com/yixin98/ED2/tree/new_plasticity

References

Anderson-Teixeira, K. J., Wang, M. M. H., McGarvey, J. C., & LeBauer, D. S. (2016). Carbon dynamics of mature and regrowth tropical forests derived from a pantropical database (TropForC-db). *Global Change Biology*, *22*, 1690–1709. https://doi.org/10.5061/dryad.t516f

Avramov, S., Pemac, D., & Tucić, B. (2007). Phenotypic plasticity in response to an irradiance gradient in Iris pumila: Adaptive value and evolutionary constraints. *Plant Ecology*, *190*(2), 275–290. https://doi.org/10.1007/s11258-006-9207-3

Batterman, S. A., Hedin, L. O., Van Breugel, M., Ransijn, J., Craven, D. J., & Hall, J. S. (2013). Key role of symbiotic dinitrogen fixation in tropical forest secondary succession. *Nature*, *502*(7470), 224–227. https://doi.org/10.1038/nature12525

Bogan, S. A., Antonarakis, A. S., & Moorcroft, P. R. (2019). Imaging spectrometry-derived estimates of regional ecosystem composition for the Sierra Nevada, California. *Remote Sensing of Environment*, *228*, 14–30. https://doi.org/10.1016/j.rse.2019.03.031

Butler, E. E., Wythers, K. R., Flores-Moreno, H., Ricciuto, D. M., Datta, A., Banerjee, A., Atkin, O. K., Kattge, J., Thornton, P. E., Anand, M., Burrascano, S., Byun, C., Cornelissen, J. H. C., Forey, E., Jansen, S., Kramer, K., Minden, V., & Reich, P. B. (2022). Increasing Functional Diversity in a Global Land Surface Model Illustrates Uncertainties Related to Parameter Simplification. *Journal of Geophysical Research: Biogeosciences*, *127*(3). https://doi.org/10.1029/2021jg006606

Camac, J. S., Condit, R., FitzJohn, R. G., McCalman, L., Steinberg, D., Westoby, M., Joseph Wright, S., & Falster, D. S. (2018). Partitioning mortality into growth-dependent and growth-independent hazards across 203 tropical tree species. *Proceedings of the National Academy of Sciences of the United States of America*, *115*(49), 12459–12464. https://doi.org/10.1073/pnas.1721040115

Cano, I. M., Muller-Landau, H. C., Joseph Wright, S., Bohlman, S. A., & Pacala, S. W. (2019).

838 Tropical tree height and crown allometries for the Barro Colorado Nature Monument,
839 Panama: A comparison of alternative hierarchical models incorporating interspecific
840 variation in relation to life history traits. *Biogeosciences*, *16*(4), 847–862.
841 https://doi.org/10.5194/bg-16-847-2019
842 Cavaleri, M. A., Oberbauer, S. F., Clark, D. B., Clark, D. A., & Ryan, M. G. (2010). Height is more
843 important than light in determining leaf morphology in a tropical forest. *Ecology*, *91*(6),
844 1730–1739. https://doi.org/10.1890/09-1326.1
845 Chazdon, R. L., & Fetcher, N. (1984). Photosynthetic Light Environments in a Lowland Tropical
846 Rain Forest in Costa Rica. *The Journal of Ecology*, *72*(2), 553–564.
847 https://doi.org/10.2307/2260066
848 Chmura, D. J., Modrzyński, J., Chmielarz, P., & Tjoelker, M. G. (2017). Plasticity in seedling
849 morphology, biomass allocation and physiology among ten temperate tree species in
850 response to shade is related to shade tolerance and not leaf habit. *Plant Biology*, *19*(2),
851 172–182. https://doi.org/10.1111/plb.12531
852 Clark, D. B., Clark, D. A., Rich, P. M., Weiss, S., & Oberbauer, S. F. (1996). Landscape-scale
853 evaluation of understory light and canopy structure: methods and application in a
854 neotropical lowland rain forest. *Canadian Journal of Forest Research*, *26*, 747–757.
855 Condit, R., Pérez, R., Lao, S., Aguilar, S., & Hubbell, S. P. (2017). Demographic trends and climate
856 over 35 years in the Barro Colorado 50 ha plot. *Forest Ecosystems*, *4*(1), 1–13.
857 https://doi.org/10.1186/s40663-017-0103-1
858 Condit, R., & Rüger, N. (2022). *Demographic variation and demographic niches of trees species*
859 *in the Barro Colorado Forest*. https://doi.org/10.1101/2022.07.07.499151
860 Coste, S., Roggy, J. C., Garraud, L., Heuret, P., Nicolini, E., & Dreyer, E. (2009). Does ontogeny
861 modulate irradiance-elicited plasticity of leaf traits in saplings of rain-forest tree species? A
862 test with Dicorynia guianensis and Tachigali melinonii (Fabaceae, Caesalpinioideae). *Annals*
863 *of Forest Science*, *66*(7), 709–709. https://doi.org/10.1051/forest/2009062
864 Dang-Le, A. T., Edelin, C., & Le-Cong, K. (2013). Ontogenetic variations in leaf morphology of the
865 tropical rain forest species Dipterocarpus alatus Roxb. ex G. Don. *Trees - Structure and*
866 *Function*, *27*(3), 773–786. https://doi.org/10.1007/s00468-012-0832-2

867 Denslow, J. S. (1987). Tropical Rainforest Gaps and Tree Species Diversity. *Annual Review of*
868 *Ecology and Systematics*, *18*, 431–451.
869 Detto, M., Asner, G. P., Muller-Landau, H. C., & Sonnentag, O. (2015). Spatial variability in
870 tropical forest leaf area density from multireturn lidar and modeling. *Journal of*
871 *Geophysical Research: Biogeosciences*, *120*, 707–723.
872 https://doi.org/10.1002/2014JG002774.Received
873 Detto, M., Levine, J. M., & Pacala, S. W. (2021). Maintenance of high diversity in mechanistic
874 forest dynamics models of competition for light. *Ecological Monographs*, *92*(2).
875 https://doi.org/10.1002/ecm.1500
876 Detto, M., & Pacala, S. W. (2022). Plant hydraulics, stomatal control, and the response of a
877 tropical forest to water stress over multiple temporal scales. *Global Change Biology*,
878 *28*(14), 4359–4376. https://doi.org/10.1111/gcb.16179
879 Detto, M., Wright, S. J., Calderón, O., & Muller-Landau, H. C. (2018). Resource acquisition and
880 reproductive strategies of tropical forest in response to the El Niño-Southern Oscillation.
881 *Nature Communications*, *9*(1), 1–8. https://doi.org/10.1038/s41467-018-03306-9
882 Detto, M., & Xu, X. (2020). Optimal leaf life strategies determine Vc,max dynamic during
883 ontogeny. *New Phytologist*, *228*(1), 361–375. https://doi.org/10.1111/nph.16712
884 DeWitt, T. J., Sih, A., & Wilson, D. S. (1998). Costs and limits of phenotypic plasticity. *Trends in*
885 *Ecology and Evolution*, *13*(2), 77–81. https://doi.org/10.1016/S0169-5347(97)01274-3
886 Finegan, B. (1984). Forest succession. *Nature*, *312*(8), 109–114.
887 Food and Agriculture Organization of the United Nations. (2010). Global forest resources
888 assessment 2010: Main report. *FAO Forestry Paper 163*.
889 https://www.fao.org/4/i1757e/i1757e.pdf
890 Kitajima, K. (1994). Relative importance of photosynthetic traits and allocation patterns as
891 correlates of seedling shade tolerance of 13 tropical trees. *Oecologia*, *98*(3–4), 419–428.
892 https://doi.org/10.1007/BF00324232
893 Koven, C. D., Knox, R. G., Fisher, R. A., Fisher, R. A., Chambers, J. Q., Chambers, J. Q.,
894 Christoffersen, B. O., Davies, S. J., Detto, M., Detto, M., Dietze, M. C., Faybishenko, B.,
895 Holm, J., Huang, M., Kovenock, M., Kueppers, L. M., Kueppers, L. M., Lemieux, G.,

Massoud, E., … Xu, C. (2020). Benchmarking and parameter sensitivity of physiological and vegetation dynamics using the Functionally Assembled Terrestrial Ecosystem Simulator (FATES) at Barro Colorado Island, Panama. *Biogeosciences*, *17*(11), 3017–3044. https://doi.org/10.5194/bg-17-3017-2020

Lamour, J., Davidson, K. J., Ely, K. S., Le Moguédec, G., Anderson, J. A., Li, Q., Calderón, O., Koven, C. D., Wright, S. J., Walker, A. P., Serbin, S. P., & Rogers, A. (2023). The effect of the vertical gradients of photosynthetic parameters on the CO2 assimilation and transpiration of a Panamanian tropical forest. *New Phytologist*, *238*, 2345–2362. https://doi.org/10.1111/nph.18901

Liu, Y., Dawson, W., Prati, D., Haeuser, E., Feng, Y., & Van Kleunen, M. (2016). Does greater specific leaf area plasticity help plants to maintain a high performance when shaded? *Annals of Botany*, *118*(7), 1329–1336. https://doi.org/10.1093/aob/mcw180

Lloyd, J., Patiño, S., Paiva, R. Q., Nardoto, G. B., Quesada, C. A., Santos, A. J. B., Baker, T. R., Brand, W. A., Hilke, I., Gielmann, H., Raessler, M., Luizão, F. J., Martinelli, L. A., & Mercado, L. M. (2010). Optimisation of photosynthetic carbon gain and within-canopy gradients of associated foliar traits for Amazon forest trees. *Biogeosciences*, *7*(6), 1833–1859. https://doi.org/10.5194/bg-7-1833-2010

Longo, M., Knox, R. G., Levine, N. M., Swann, A. L. S., Medvigy, D. M., Dietze, M. C., Kim, Y., Zhang, K., Bonal, D., Burban, B., Camargo, P. B., Hayek, M. N., Saleska, S. R., Da Silva, R., Bras, R. L., Wofsy, S. C., & Moorcroft, P. R. (2019). The biophysics, ecology, and biogeochemistry of functionally diverse, vertically and horizontally heterogeneous ecosystems: The Ecosystem Demography model, version 2.2-Part 2: Model evaluation for tropical South America. *Geoscientific Model Development*, *12*(10), 4347–4374. https://doi.org/10.5194/gmd-12-4347-2019

Longo, M., Knox, R. G., Medvigy, D. M., Levine, N. M., Dietze, M. C., Kim, Y., Swann, A. L. S., Zhang, K., Rollinson, C. R., Bras, R. L., Wofsy, S. C., & Moorcroft, P. R. (2019). The biophysics, ecology, and biogeochemistry of functionally diverse, vertically and horizontally heterogeneous ecosystems: The Ecosystem Demography model, version 2.2-Part 1: Model description. *Geoscientific Model Development*, *12*(10), 4309–4346.

https://doi.org/10.5194/gmd-12-4309-2019

McIntyre, P. J., & Strauss, S. Y. (2014). Phenotypic and transgenerational plasticity promote local adaptation to sun and shade environments. *Evolutionary Ecology*, *28*(2), 229–246. https://doi.org/10.1007/s10682-013-9670-y

Moorcroft, P. R., Hurtt, G. C., & Pacala, S. W. (2001). A method for scaling vegetation dynamics: The ecosystem demography model (ED). *Ecological Monographs*, *71*(4), 557–586. https://doi.org/10.1890/0012-9615(2001)071[0557:AMFSVD]2.0.CO;2

Needham, J. F., Dey, S., Koven, C. D., Fisher, R. A., Knox, R. G., Lamour, J., Lemieux, G., Longo, M., Rogers, A., & Holm, J. (2025). Vertical canopy gradients of respiration drive plant carbon budgets and leaf area index. *New Phytologist*. https://doi.org/10.1111/nph.20423

Niinemets, Ü., Keenan, T. F., & Hallik, L. (2015). A worldwide analysis of within-canopy variations in leaf structural, chemical and physiological traits across plant functional types. *New Phytologist*, *205*(3), 973–993. https://doi.org/10.1111/nph.13096

Osunkoya, O. O., Ash, J. E., Hopkins, M. S., Andrew, W., Osunkoya, O., Ash, J. E., & Hopkinst, M. S. (1994). Influence of Seed Size and Seedling Ecological Attributes on Shade-Tolerance of Rain- Forest Tree Species in Northern Queensland. *Journal of Ecology*, *82*(1), 149–163.

Pan, Y., Birdsey, R. A., Fang, J., Houghton, R., Kauppi, P. E., Kurz, W. A., & Philips, O. L. (2011). A Large and Persistent Carbon Sink in the World's Forests. *Science*, *333*, 988–993. https://doi.org/10.1126/science.1204588

Pappas, C., Fatichi, S., & Burlando, P. (2016). Modeling terrestrial carbon and water dynamics across climatic gradients: Does plant trait diversity matter? *New Phytologist*, *209*(1), 137–151. https://doi.org/10.1111/nph.13590

Pavlick, R., Drewry, D. T., Bohn, K., Reu, B., & Kleidon, A. (2013). The Jena Diversity-Dynamic Global Vegetation Model (JeDi-DGVM): a diverse approach to representing terrestrial biogeography and biogeochemistry based on plant functional trade-offs. *Biogeosciences*, *10*(6), 4137–4177. https://doi.org/10.5194/bg-10-4137-2013

Poorter, H., Niinemets, Ü., Ntagkas, N., Siebenkäs, A., Mäenpää, M., Matsubara, S., & Pons, T. L. (2019). A meta-analysis of plant responses to light intensity for 70 traits ranging from molecules to whole plant performance. *New Phytologist*, *223*(3), 1073–1105.

954 https://doi.org/10.1111/nph.15754
955 Poorter, L., Castilho, C. V., Schietti, J., Oliveira, R. S., & Costa, F. R. C. (2018). Can traits predict
956 individual growth performance? A test in a hyperdiverse tropical forest. *New Phytologist*,
957 *219*(1), 109–121. https://doi.org/10.1111/nph.15206
958 Poorter, L., Craven, D., Jakovac, C. C., van der Sande, M. T., Amissah, L., Bongers, F., Chazdon, R.
959 L., Farrior, C. E., Kambach, S., Meave, J. A., Muñoz, R., Norden, N., Rüger, N., van Breugel,
960 M., María Almeyda Zambrano, A., Amani, B., Luis Andrade, J., S Brancalion, P. H.,
961 Broadbent, E. N., … Hérault, B. (2021). Multidimensional tropical forest recovery. *Science*,
962 1370–1376. https://www.science.org
963 Pugh, T. A. M., Lindeskog, M., Smith, B., Poulter, B., Arneth, A., Haverd, V., & Calle, L. (2019).
964 Role of forest regrowth in global carbon sink dynamics. *Proceedings of the National*
965 *Academy of Sciences of the United States of America*, *116*(10), 4382–4387.
966 https://doi.org/10.1073/pnas.1810512116
967 Reich, P. B. (2014). The world-wide "fast-slow" plant economics spectrum: a traits manifesto.
968 *The Journal of Ecology*, *102*(2), 275–301.
969 Reich, P. B., Stefanski, A., Rich, R. L., Sendall, K. M., Wei, X., Zhao, C., Hou, J., Montgomery, R. A.,
970 & Bermudez, R. (2021). Assessing the relevant time frame for temperature acclimation of
971 leaf dark respiration: A test with 10 boreal and temperate species. *Global Change Biology*,
972 *27*, 2945–2958. https://doi.org/10.1111/gcb.15609
973 Ren, Y., Wang, H., Harrison, S. P., Prentice, I. C., Atkin, O. K., Smith, N. G., Mengoli, G., Stefanski,
974 A., & Reich, P. B. (2024). Reduced global plant respiration due to the acclimation of leaf
975 dark respiration coupled with photosynthesis. *New Phytologist*, *241*(2), 578–591.
976 https://doi.org/10.1111/nph.19355
977 Rius, B. F., Filho, J. P. D., Fleischer, K., Hofhansl, F., Blanco, C. C., Rammig, A., Domingues, T. F.,
978 & Lapola, D. M. (2023). Higher functional diversity improves modeling of Amazon forest
979 carbon storage. *Ecological Modelling*, *481*.
980 https://doi.org/10.1016/j.ecolmodel.2023.110323
981 Rüger, N., Condit, R., Dent, D. H., DeWalt, S. J., Hubbell, S. P., Lichstein, J. W., Lopez, O. R.,
982 Wirth, C., & Farrior, C. E. (2020). Demographic trade-offs predict tropical forest dynamics.

Science, *368*(6487), 165–168. https://doi.org/10.1126/science.aaz4797

Sakschewski, B., Von Bloh, W., Boit, A., Poorter, L., Peña-Claros, M., Heinke, J., Joshi, J., & Thonicke, K. (2016). Resilience of Amazon forests emerges from plant trait diversity. *Nature Climate Change*, *6*(11), 1032–1036. https://doi.org/10.1038/nclimate3109

Shevliakova, E., Pacala, S. W., Malyshev, S., Hurtt, G. C., Milly, P. C. D., Caspersen, J. P., Sentman, L. T., Fisk, J. P., Wirth, C., & Crevoisier, C. (2009). Carbon cycling under 300 years of land use change: importance of the secondary vegetation sink. *Global Biogeochemical Cycles*, *23*(2). https://doi.org/10.1029/2007GB003176

Siefert, A., Violle, C., Chalmandrier, L., Albert, C. H., Taudiere, A., Fajardo, A., Aarssen, L. W., Baraloto, C., Carlucci, M. B., Cianciaruso, M. V., de L. Dantas, V., de Bello, F., Duarte, L. D. S., Fonseca, C. R., Freschet, G. T., Gaucherand, S., Gross, N., Hikosaka, K., Jackson, B., … Wardle, D. A. (2015). A global meta-analysis of the relative extent of intraspecific trait variation in plant communities. *Ecology Letters*, *18*(12), 1406–1419. https://doi.org/10.1111/ele.12508

Sterck, F. J., Duursma, R. A., Pearcy, R. W., Valladares, F., Cieslak, M., & Weemstra, M. (2013). Plasticity influencing the light compensation point offsets the specialization for light niches across shrub species in a tropical forest understorey. *Journal of Ecology*, *101*(4), 971–980. https://doi.org/10.1111/1365-2745.12076

United Nations General Assembly. (2015). *A/RES/70/1 - Transforming our world: The 2030 agenda for sustainable development*. https://doi.org/10.4324/9781843146575-59

Valladares, F., Wright, S. J., Lasso, E., Kitajima, K., & Pearcy, R. W. (2000). Plastic phenotypic response to light of 16 congeneric shrubs from a panamanian rainforest. *Ecology*, *81*(7), 1925–1936. https://doi.org/10.1890/0012-9658(2000)081[1925:PPRTLO]2.0.CO;2

Wen, S., Fetcher, N., & Zimmerman, J. K. (2008). Acclimation of tropical tree species to hurricane disturbance: ontogenetic differences. *Tree Physiology*, *28*, 935–946.

Wright, S. J., Kitajima, K., Kraft, N. J. B., Reich, P. B., Wright, I. J., Bunker, D. E., Condit, R., Dalling, J. W., Davies, S. J., DíAz, S., Engelbrecht, B. M. J., Harms, K. E., Hubbell, S. P., Marks, C. O., Ruiz-Jaen, M. C., Salvador, C. M., & Zanne, A. E. (2010). Functional traits and the growth-mortality trade-off in tropical trees. *Ecology*, *91*(12), 3664–3674.

https://doi.org/10.1890/09-2335.1

Xu, X., Medvigy, D., Joseph Wright, S., Kitajima, K., Wu, J., Albert, L. P., Martins, G. A., Saleska, S. R., & Pacala, S. W. (2017). Variations of leaf longevity in tropical moist forests predicted by a trait-driven carbon optimality model. *Ecology Letters*, *20*, 1097–1106. https://doi.org/10.1111/ele.12804

Xu, X., Medvigy, D., Powers, J. S., Becknell, J. M., & Guan, K. (2016). Diversity in plant hydraulic traits explains seasonal and inter-annual variations of vegetation dynamics in seasonally dry tropical forests. *The New Phytologist*, *212*(1), 80–95. https://doi.org/10.1111/nph.14009

Xu, X., van der Sleen, P., Groenendijk, P., Vlam, M., Medvigy, D., Moorcroft, P., Petticord, D., Ma, Y., & Zuidema, P. A. (2024). Constraining long-term model predictions for woody growth using tropical tree rings. *Global Change Biology*, *30*(1). https://doi.org/10.1111/gcb.17075

Yaffar, D., Lugli, L. F., Wong, M. Y., Norby, R. J., Addo-Danso, S. D., Arnaud, M., Cordeiro, A. L., Dietterich, L. H., Diaz-Toribio, M. H., Lee, M. Y., Ghimire, O. P., Smith-Martin, C. M., Toro, L., Andersen, K., McCulloch, L. A., Meier, I. C., Powers, J. S., Sanchez-Julia, M., Soper, F. M., & Cusack, D. F. (2024). Tropical root responses to global changes: A synthesis. *Global Change Biology*, *30*(7). https://doi.org/10.1111/gcb.17420

Yang, X., Li, R., Jablonski, A., Stovall, A., Kim, J., Yi, K., Ma, Y., Beverly, D., Phillips, R., Novick, K., Xu, X., & Lerdau, M. (2023). Leaf angle as a leaf and canopy trait: Rejuvenating its role in ecology with new technology. *Ecology Letters*, *26*(6), 1005–1020. https://doi.org/10.1111/ele.14215